frontiers

Supplementary Material

1 Supplementary Methods

Samples for optical characterization of DOM were filtered in the same manner than those for DOC. Fluorescence was obtained for the excitation/emission pairs described by (Coble, 1996) using a Perkin Elmer LS55 spectrofluorometer. Daily produced Milli-Q water signal was used as blank and the fluorescence data was transformed to Raman units (RU) by dividing each signal by the integral of the Raman scatter peak (Lawaetz and Stedmon, 2009). Humic fluorescence was calculated as the sum of each humic peak fluorescence (i.e. peaks "A", "C" and "M") and is given in RU per mmol of DOC. Absorbance spectra (250-700 nm) were obtained against Milli-Q water using a Varian Cary 100 Bio UV-Vis spectrophotometer. Absorbance was baseline corrected by subtracting the mean absorbance in the range 600-700 nm. We report the ratio a300:a400 between the absorption coefficient at 300 nm and that at 400 nm, which is negatively correlated with humification (Li and Hur, 2017).

For the oxygen consumption estimates, we considered a respiratory quotient (molar ratio of CO_2 produced to O_2 consumed) of 0.89, typical of planktonic material (Del Giorgio and Williams, 2005), to calculate the oxygen consumption derived from the observed TOC reductions throughout the experiment. The microbial respiratory reductions were estimated based on the model from Cram et al. (2018) and using the highest (more pessimistic scenario) oxygen semi-saturation constant reported (DeVries and Weber, 2017).

2 Supplementary Figures and Tables

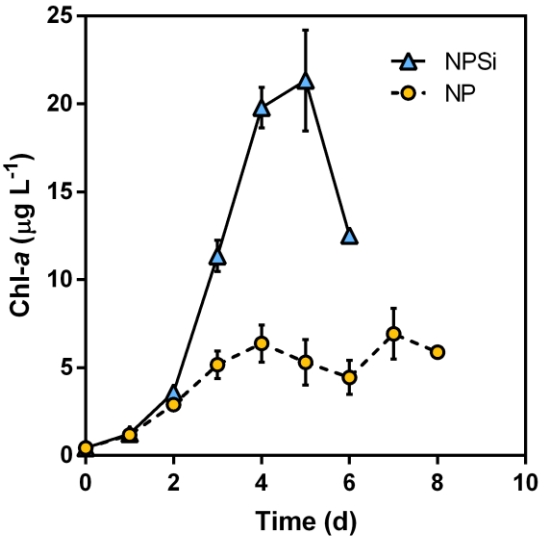

Supplementary Figure 1. Time course of Chl-a concentration during the NP and NPSi incubations. Note that NP reaches its maximum Chl-a concentration at day 7, one day after its second addition of nutrients (day 6). Data are mean and standard deviation (n=5). The last data point of each incubation is the Chl-a concentration in the mixed microcosms (see methods).

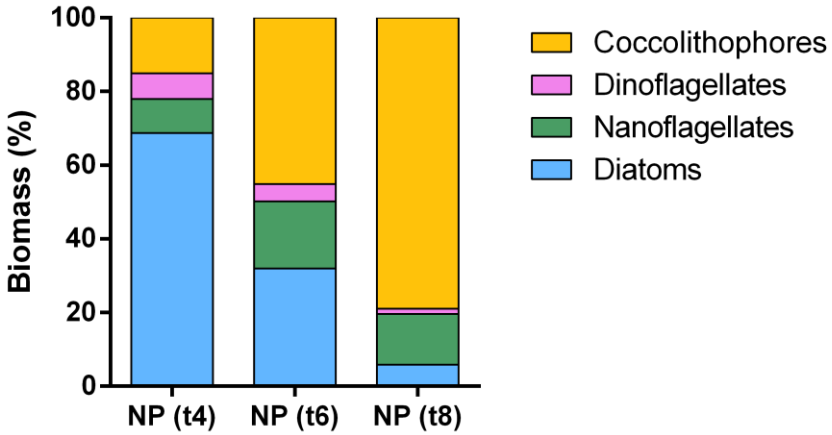

Supplementary Figure 2. Phytoplankton biomass composition at different time-points of the NP incubation showing the functional group succession associated with the exhaustion of silicate along this incubation. Data at days 4 and 6 are the mean composition of five microcosms, whereas the composition of day 8 is based on the mix of NP five microcosms. No diatom spore was detected in any of NP incubation samples.

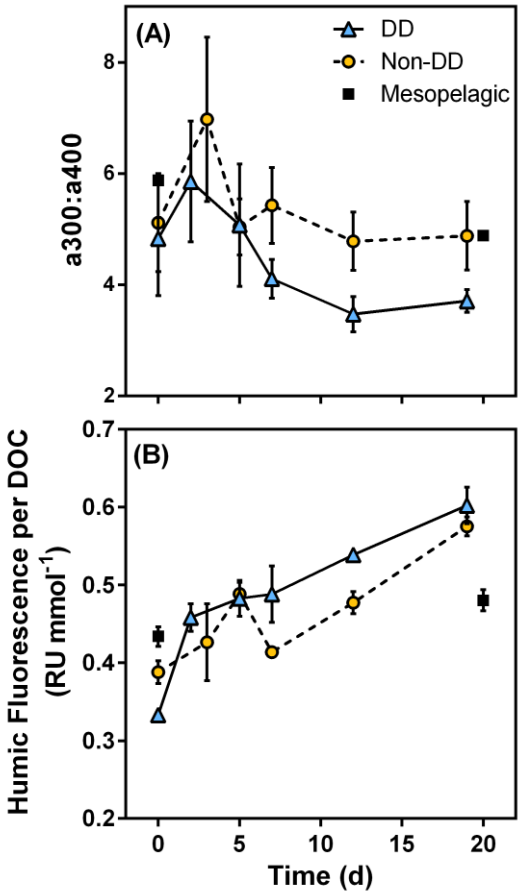

Supplementary Figure 3. Time course of two optical indices of DOM humification: The ratio a300:a400 **(A)**, negatively correlated with humification, decreases in the DD treatment as DOC accumulates (after day 5, Figure 3) and remains below the values of both the non-DD treatment and mesopelagic water at the end of the incubation. DOC-normalized humic fluorescence **(B)** increases similarly in both non-DD and DD treatments after day 5, indicating ongoing DOM humification even as DOC accumulates in the DD treatment (Figure 3).

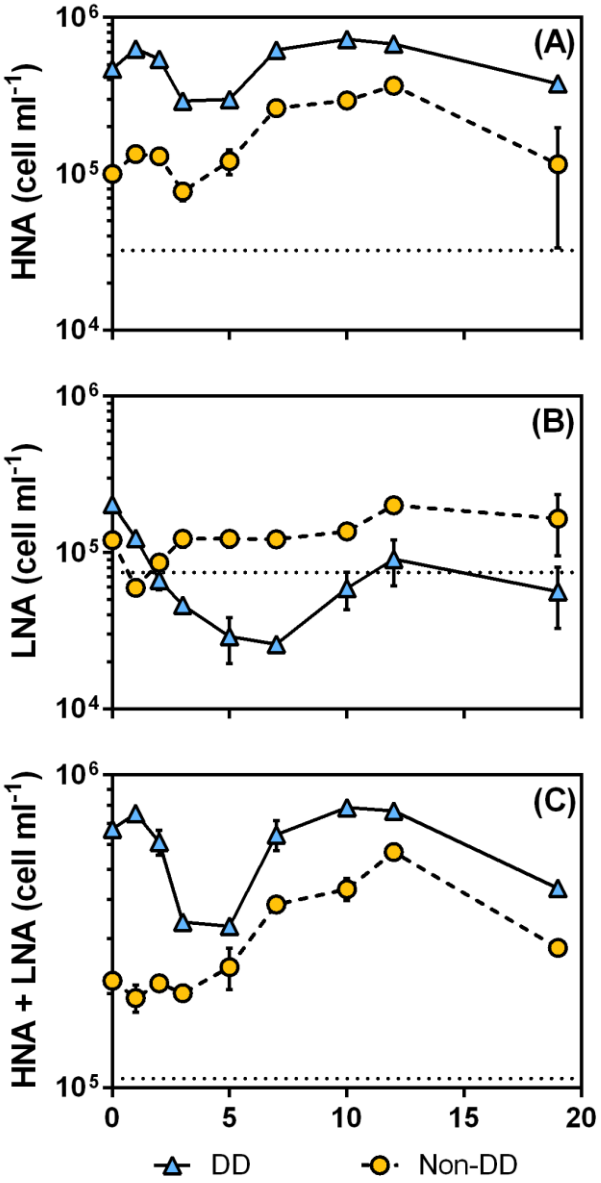

Supplementary Figure 4. Time course of FC-derived prokaryotic abundances (cell ml-1), divided into subpopulations as described in methods: High-Nucleic Acid (HNA) bacteria **(A)**, Low-Nucleic Acid (LNA) bacteria **(B)** and total bacterial abundances **(C)**. Mean cell abundance of mesopelagic water prior to POM addition is shown as a dotted line in each panel.

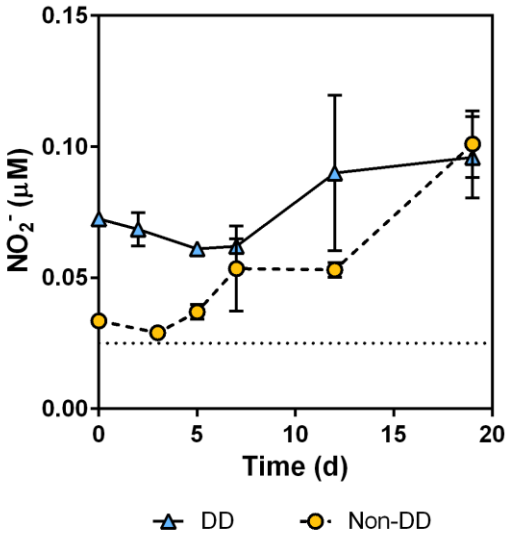

Supplementary Figure 5. Time course of nitrite concentrations in each treatment. Concentration in mesopelagic water prior to POM additions is represented as a dotted line.

Supplementary Table 1. Concentrations (mean ± sd), consumptions, additions and N:P ratio of nutrients for the light incubations (NP and NPSi). Note the extremely low N:P ratio at the end of the NPSi incubation, indicating N-limiting conditions.

	Nitrate (µmol L^{-1})	**Phosphate (µmol L^{-1})**	**Silicate (µmol L^{-1})**	**N:P (mol:mol)**
Surface SW	0.14 ± 0.00	0.028 ± 0.001	0.79 ± 0.02	4.9
NP (t0)	23.27 ± 0.45	1.386 ± 0.006	0.82 ± 0.05	16.8
NPSi (t0)	23.26 ± 0.46	1.386 ± 0.012	20.10 ± 0.22	16.8
NP (t8)	23.84 ± 0.53	1.402 ± 0.174	0.27 ± 0.10	17.0
NPSi (t6)	0.23 ± 0.01	0.466 ± 0.235	2.58 ± 0.30	0.5
NP consumption	22.56	1.34	0.52	16.8
NPSi consumption	23.02	0.92	17.52	25.0
Total added to NP	46.26	2.717	-	17.0
Total added to NPSi	23.12	1.358	19.31	17.0

3 Supplementary References

Coble, P. G. (1996). Characterization of marine and terrestrial DOM in seawater using excitation-emission matrix spectroscopy. *Mar. Chem.* 51, 325–346. doi:10.1016/0304-4203(95)00062-3.

Cram, J. A., Weber, T., Leung, S. W., McDonnell, A. M. P., Liang, J. H., and Deutsch, C. (2018). The Role of Particle Size, Ballast, Temperature, and Oxygen in the Sinking Flux to the Deep Sea. *Global Biogeochem. Cycles* 32, 858–876. doi:10.1029/2017GB005710.

Del Giorgio, P., and Williams, P. (2005). *Respiration in Aquatic Ecosystems*. , eds. P. del Giorgio and P. Williams Oxford University Press doi:10.1093/acprof:oso/9780198527084.001.0001.

DeVries, T., and Weber, T. (2017). The export and fate of organic matter in the ocean: New constraints from combining satellite and oceanographic tracer observations. *Global Biogeochem. Cycles* 31, 535–555. doi:10.1002/2016GB005551.

Lawaetz, A. J., and Stedmon, C. A. (2009). Fluorescence intensity calibration using the Raman scatter peak of water. *Appl. Spectrosc.* 63, 936–940. doi:10.1366/000370209788964548.

Li, P., and Hur, J. (2017). Utilization of UV-Vis spectroscopy and related data analyses for dissolved organic matter (DOM) studies: A review. *Crit. Rev. Environ. Sci. Technol.* 47, 131–154. doi:10.1080/10643389.2017.1309186.